Preparation and Permeation Characterization of β-Zeolite-Incorporated Composite Membranes

Zhen Huang,[1,2] Jun-Feng Su,[2] Xiao-Qun Su,[2] Yu-Hua Guo,[2] Li-Jun Teng,[2] Chuan Min Yang[2]

[1]*Tianjin Key Laboratory of Food and Biotechnology, Tianjin University of Commerce, Tianjin 300134, China*
[2]*Department of Packaging Engineering, Institute of Materials Science and Chemical Engineering, Tianjin University of Commerce, Tianjin 300134, China*

Received 17 February 2008; accepted 13 September 2008
DOI 10.1002/app.29361
Published online 18 December 2008 in Wiley InterScience (www.interscience.wiley.com).

ABSTRACT: In this work, several β-zeolite-incorporated polymer composite membranes were fabricated with the solution-casting method. The zeolite loadings were 10, 20, and 30 wt %, respectively. Scanning electron microscopy characterization showed that the zeolite particles could be uniformly distributed in the whole polymer matrix. Gas permeation results demonstrated that after the incorporation of the same β-zeolite, the polyimide exhibited a significant increase in gas permeability but a decrease in permselectivity, and both were quite pronounced at high zeolite loadings; this resulted from the loose structure that formed. The poly(ether sulfone) composite membranes showed obvious increases in both permeability and selectivity, and the permeability increase was considerably greater at higher zeolite loadings. The permselectivity increase could possibly be attributed to the pore sieving and preferential adsorption of β-zeolite entities for the test gases as the heat treatment may have resulted in the formation of a defect-free microstructure. However, breakthrough of the upper-bound line was not achieved for these composite membranes, as reflected by Robeson plots. Our results suggest that changes in membrane performance not only are attributable to the properties and content of β-zeolite particles but also depend on the heterogeneous microstructure created by zeolite entities. © 2008 Wiley Periodicals, Inc. J Appl Polym Sci 112: 9–18, 2009

Key words: composites; gas permeation; poly(ether sulfones); polyimides; zeolites

INTRODUCTION

Zeolite materials possess unique transport properties and adsorption properties because they have well-defined crystalline frameworks with the pore size at the molecular level. β-Zeolite, a large-pore and high-silica zeolite with a typical Si/Al ratio of 10–25, possesses a three-dimensional, 12-ring interconnected channel system with topographical pore diameters of 0.71–0.73 nm.[1] A number of studies have shown that β-zeolite is of great petrochemical interest as a good catalyst for chemical reactions.[2–5] Furthermore, several research groups have attempted to synthesize highly crystalline β-zeolite membranes for separation and catalysis.[6–8] The resultant membranes have good permeation selectivity for several organic/water mixtures[6] or structural isomers and stereoisomers[7] because of preferential adsorption of one component over the other in the membranes. However, single-gas permeance results have shown that the ideal selectivities of H_2/N_2, H_2/n-C4, and H_2/i-C4 for these membranes are less than the Knudsen selectivities, and this is generally not expected for zeolite pores.[6] These results may be due to the competing effects of adsorption and diffusion in zeolite pores for gas molecules of different sizes, and larger molecules have lower diffusivities but higher adsorption coverage than smaller molecules. Thus, adsorption investigations for lots of compounds have been carried out on this type of zeolite.[9–11] Because of its sinusoidal pore structure and selective adsorption capacity, β-zeolite performs very well in separating C_5–C_8 alkane isomers or effectively discriminating the monobranched isomer from the dibranched one.[9,10] Besides, β-zeolite is also a good candidate for applications in fuel gas separation as well as natural gas and landfill gas purification.[11] Recently, β-zeolite has received attention for the preparation of polymer-based composite membranes for gas separation applications.[12–16] Li et al.[12] fabricated dual-layer, hollow-fiber membranes by embedding β-zeolite into the polymer matrix, and enhanced O_2/N_2 and CO_2/CH_4 selectivity of around 10–20% was achieved with respect to the dense neat

Correspondence to: Z. Huang (huang900@yahoo.com).
Contract grant sponsor: National Key Technologies R & D Program of China; contract grant number: 2006BAD05A05.
Contract grant sponsor: Tianjin University of Commerce; contract grant number: R-060102Q.

poly(ether sulfone) (PES) film. Similarly, enhanced selectivity for He/N_2 and O_2/N_2 separation resulted from the incorporation of β-zeolite into the polysulfone-selective layer.[13] Later, these authors employed β-zeolite embedded in the polymer matrix as a novel precursor for fabricating hollow carbon fiber membranes.[14] The newly developed carbon-based composite membranes have exhibited significantly enhanced selectivity for O_2/N_2 and CO_2/CH_4 pairs because of the integrating function of the embedded β-zeolite. Very excitingly, β-zeolite-incorporated PES composite membranes have exhibited pronounced permeation performance with an ideal selectivity of CO_2/CH_4 over 6 times greater than that of pure PES.[15] Moreover, β-zeolite has also been successfully embedded into multilayered poly(vinyl alcohol) composite membrane for ethanol dehydration by means of pervaporation, subsequently leading to both high separation factors and high fluxes.[17] The progress of these composite membranes, composed of homogeneously interpenetrating polymeric and inorganic particle matrices, suggests that the addition of a zeolite filler provides the potential to increase the performance of existing polymeric membranes by increasing the flux of the more permeable gas while maintaining or improving the pure polymer's selectivity, and the performance enhancement gained may be due to the addition of Knudsen diffusion and selective adsorption to the solution–diffusion mechanism that predominates in nonporous pure polymer membranes.[16] These advances encourage laboratory-scale studies on fabrication and separation applications of β-zeolite-embedded composite membranes for understanding the separation mechanism and subsequent industrial practices.

In this work, we fabricated a series of polymer-based composite membranes for gas separation by incorporating self-synthesized β-zeolite. Two glassy polymers of PES and polyimide (PI) were used as the matrices for zeolite incorporation as they exhibit great application potential for natural gas separation.[18] Thus, we have not only provided the straightforward experimental results about the use of β-zeolite in modifying PI membrane performance, but we have also reexamined previous work about the performance of PES–β-zeolite composite membranes to explore the potential of using these composite membranes for any practical application. The zeolite-integrated composite membranes were fabricated by a solution-casting protocol, and this was followed by morphology examinations with scanning electron microscopy (SEM). The pure gas permeation measurements for these polymer-based composite membranes were carried out at 35°C with a variable-pressure, constant-volume method. These experimentally obtained permeation data were analyzed in terms of the zeolite properties and through the Robeson approach as well.

EXPERIMENTAL

β-Zeolite

The aluminum-containing β-zeolite used in this study was self-synthesized with a typical molar reaction gel composition (1.5 Na_2O/1.00 Al_2O_3/10 tetraethylammonium (TEAOH)/30 SiO_2/245 H_2O) in our laboratory at 170°C in 96 h by the hydrothermal method.[19] The calcined sample was characterized by a few techniques: X-ray diffraction (XRD), SEM, and nitrogen adsorption/desorption analysis. Powder XRD spectra, recorded on a Shimadzu XRD-6000 spectrometer (Kyoto, Japan) using Cu Kα radiation (1.5406 Å), with the samples scanned from 5 to 50° in steps of 0.02° at each point, were taken to confirm the β-zeolite structure. Nitrogen adsorption/desorption isotherms were obtained on a Quantachrome Autosorb-1 (Boynton Beach, FL) using high-purity N_2 to determine the specific surface area and pore volume. SEM examinations were performed on a JEOL JSM-6700F with conventional sample preparation and imaging techniques.

Membrane preparation

In this study, a few different β-zeolite-incorporated composite membranes were fabricated through a solution-casting method, which was similar to what was reported in our previous work.[20] The polymers used as the matrices were PES (Radel A 200, Amoco, Dusseldorf, Germany) with a glass-transition temperature (T_g) of 220°C and PI (Matrimid-5218, Ciba-Geigy, Tarrytown, NJ) with a T_g value of 320°C. The membranes fabricated at zeolite loadings of 10, 20, and 30 wt % were named PES-10, PES-20, and PES-30 and PI-10, PI-20, and PI-30, respectively. The procedure can be briefly described as follows. The dope solvent used for preparing the composite membranes was *N*-methyl-2-pyrrolidone (Merck KGaA, Darmstadt, Germany). Before use, calcined β-zeolite powder was dehydrated in an oven at a heating rate of 2.5°C/min, maintained at 250°C for 2 h, cooled naturally to room temperature, and then placed in a desiccator immediately. A desired amount of calcined β-zeolite powder was quickly weighed and dispersed in 20 g of *N*-methyl-2-pyrrolidone under agitation for 1 h and then sonicated for 5 min; this was followed by the addition of a small portion (5 g) of the polymer into the zeolite–liquid mixture. After stirring for 4 h and then sonication for 10 min, the remaining polymer was added to the resultant mixture and continuously stirred for 12 h; this resulted in a well-dispersed suspension. The

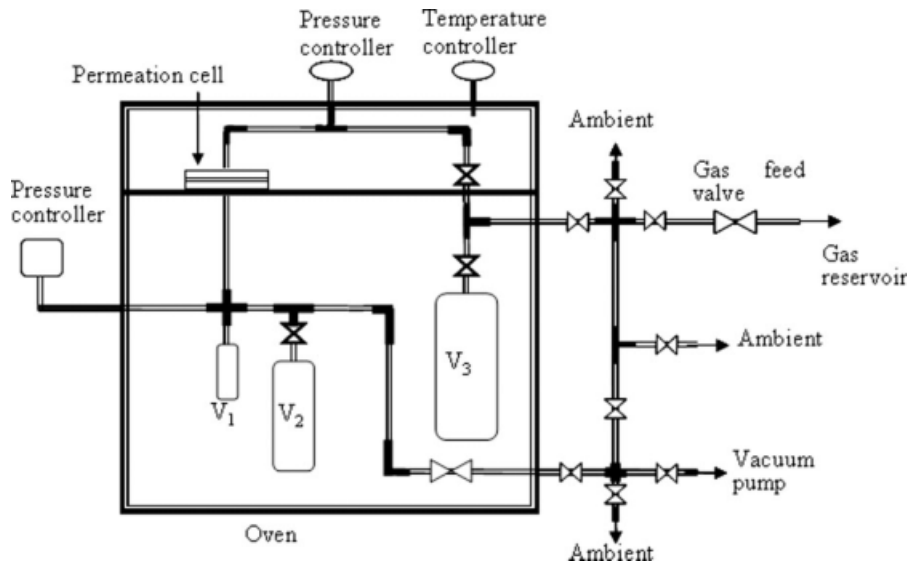

Figure 1 Schematic diagram of the single gas permeation test setup for the flat-sheet membranes.

suspension was spread onto the glass wafer and flattened with a casting knife, and it was then placed into an oven that was preheated to 150°C for the solvent evaporation. The oven then was purged with nitrogen gas for 1 h with a slight vacuum applied to the system. The oven temperature was slowly increased at 10°C/h to 200°C. After the purge was stopped, the oven was fully vacuumed and held at 200°C for around 12 h, and this was followed by annealing. The membrane annealing was carried out as follows: the oven temperature was increased from 200 to 250°C at a rate of 0.5°C/min and then maintained at 250°C for about 12 h *in vacuo*; finally, the film was taken out of the oven immediately and cooled in air.

The morphology and thickness of the resultant membranes were examined with a scanning electron microscope (JSM-6700F, JEOL). Before the SEM examinations, the samples were chilled in liquid nitrogen for at least 30 s and then folded with forceps to make a sharply broken interfacial cross section; this was followed by gold coating *in vacuo* with a sputter coater. The thickness of the dried composite membranes was determined to vary from 20 to 40 μm for PI and from 30 to 50 μm for PES, and the thickness variation was noted to be about 5 μm for each membrane sheet.

Single gas permeation test

The gas permeation properties were measured by means of a variable-pressure, constant-volume method. Figure 1 shows a schematic diagram of the experimental setup used for flat-sheet membrane gas permeation measurements. Briefly, it mainly consisted of three parts: a permeation cell, a gas feed unit [a gas reservoir, a feed valve, and a buffering vessel (V_3)], and a gas permeate unit [two vessels of different sizes (V_1 and V_2) and a vacuum pump], along with tubes, valves, and fittings of various types. A circular membrane sample was cut and tightly adhered to round aluminum adhesive tape centrally precut with a hole of a desired diameter, and this was followed by placement of the resultant tape on a stainless-steel inset sieve filter and in gas; it was tightly fixed to the permeation cell. Then, the permeation cell, made of stainless steel, was divided into two chambers (upstream feed chamber and downstream permeate chamber) by the test membrane sheet. Before we started to measure the gas permeation properties, the whole system was flushed several times with a measured amount of gas and then vacuumed for at least 12 h to remove any residual gas to obtain accurate measurements. The film sample, totally devoid of any adsorbed gases, was then in contact with the test gas at the top surface. The upstream pressure in the feed chamber was kept constant as desired, whereas the downstream pressure (p) in the permeate chamber was directly measured with an MKS 901 Baratron pressure transducer. Once the steady state was achieved, the pressure increase in the downstream chamber could be assumed to be linear with test time t. The gas permeability coefficient was thus calculated from the curve slope of the pressure at the permeate side versus time (dp/dt) in the steady state with the following equation:

$$P = 10^{10} \times \frac{273.15 p_0}{14.7T} \frac{VL}{A} \left(\frac{dp}{dt}\right) \quad (1)$$

Where P is the permeability coefficient of a membrane to gas i [barrer; 1 barrer = 10^{-10} cm^3 (STP)·

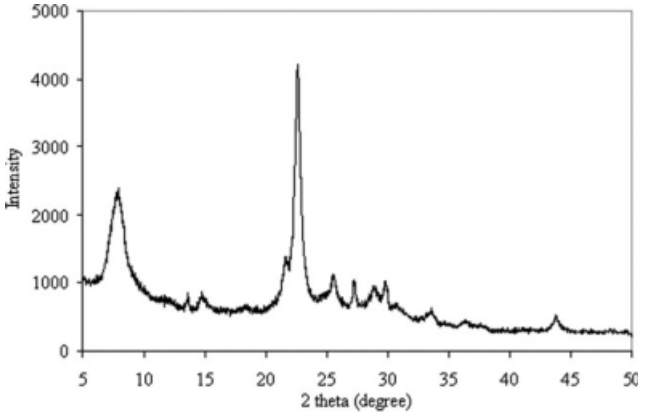

Figure 2 XRD patterns of the β-zeolite powder.

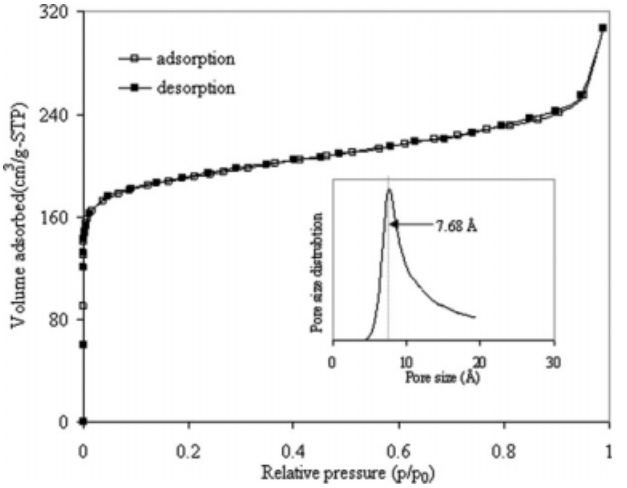

Figure 3 N_2 adsorption–desorption of the obtained β-zeolite.

cm $cm^{-2}{\cdot}cmHg^{-1}{\cdot}s^{-1}$], V is the volume of the downstream chamber (cm^3), A is the effective area of the film (cm^2), L is the thickness of the membrane (cm), p_0 is the pressure of the penetrant gas in the upstream chamber (psia), T is the absolute temperature of the measurement (K), and dp/dt is the rate of pressure measured by the pressure sensor in the low-pressure downstream chamber (cmHg/s). The ideal permselectivity of a flat-sheet membrane for pure gas A to pure gas B ($\alpha_{A/B}$) is defined as follows:

$$\alpha_{A/B} = \frac{P_A}{P_B} \tag{2}$$

where P_A and P_B are the permeability coefficient of a membrane to gas A and gas B, respectively.

The single gas permeation measurements for these β-zeolite-incorporated composite membranes were all performed on five pure gases (He, N_2, O_2, CO_2, and CH_4) at 35°C. The operational pressure was 2 atm for He gas and 10 atm for the other gases. The permeability data were all obtained by the averaging of three experimental runs.

RESULTS AND DISCUSSION

β-Zeolite properties

Figure 2 shows β-zeolite X-ray diffraction (XRD) patterns. As evidenced by the characteristic XRD peak at $2\theta = 22.5°$, which is typical of the BEA topology,[21] the zeolite used in this study was confirmed to have a pure β-zeolite structure with high crystallinity, and the amorphous silica can be ignored. Nitrogen adsorption–desorption measurements of the directly calcined sample are shown in Figure 3; the specific surface area and pore volume of β-zeolite were determined to be 665 m^2/g and 0.32 cm^3/g, respectively. The pore size distribution of β-zeolite was obtained from the desorption branch of N_2 isotherms with the Horvath–Kawazoe model, and the analysis results are also shown in Figure 3. The average pore size, taken as the peak value of the Horvath–Kawazoe pore size distribution, was determined to be 7.7 Å, which is quite close to the topographical size of 7.3 Å for β-zeolite. However, the distribution of the β-zeolite pore size is rather wide, ranging from less than 5 to over 20 Å. Figure 4 displays two SEM images for the β-zeolite used, with which the particle size and morphologies can be examined. Figure 4(a) shows that the β-zeolite particles obtained from this study were generally uniform and exhibited an average particle size of 0.20 μm, with a very narrow particle size distribution roughly ranging from 0.1 to 0.3 μm. At a high magnification [see Fig. 4(b)], these particles appeared to be agglomerations of very small β-zeolite crystals, possibly arising from the fusion and aggregation of nanosized particles during crystallization.

β-Zeolite–PI composite membranes

The single gas permeability measurements were performed on the β-zeolite-incorporated PI composite membranes at 35°C for five single gases (He, N_2, O_2, CO_2, and CH_4). The permeation results thus obtained are listed in Table I. To facilitate the comparison of permeability data, permeability enhancement (PE) is defined as follows:

$$\mathrm{PE} = \frac{P_{\mathrm{CM}} - P_{\mathrm{polym}}}{P_{\mathrm{polym}}} \tag{3}$$

where P_{polym} and P_{CM} are the permeabilities of the same gas species in the neat polymer membrane and the zeolite-embedded composite membrane, respectively. As can be seen from Table I, the single gas permeabilities of the PI membrane are significantly

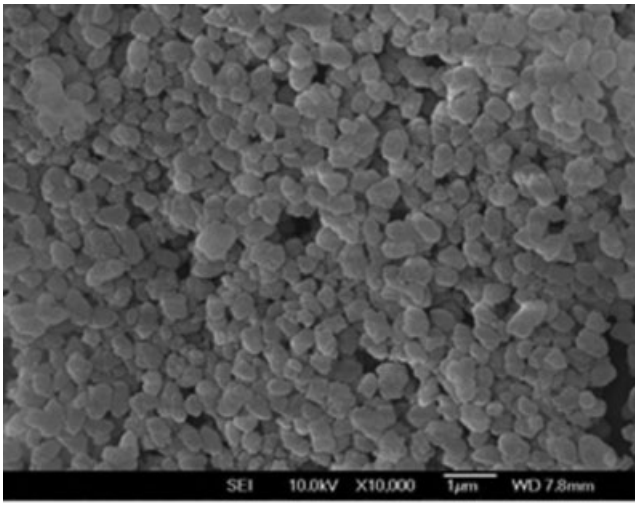

(a)

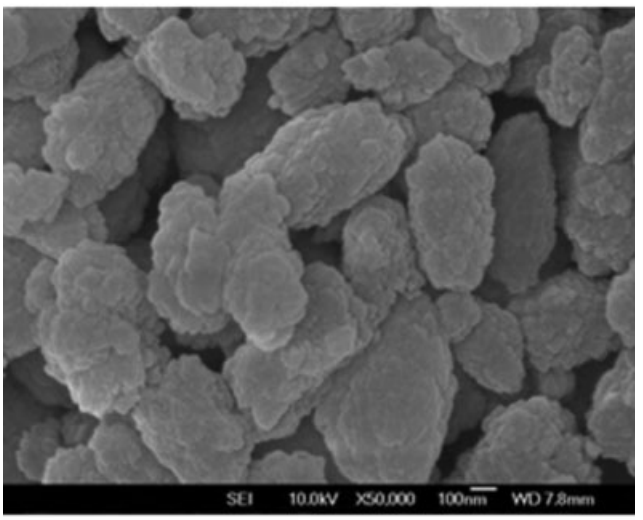

(b)

Figure 4 SEM images of the calcined β-zeolite samples at different magnifications.

improved after the incorporation of β-zeolite fillers for all the tested gases, and these permeability values are considerably higher at higher zeolite loadings. Compared to that of the neat PI counterpart, the single gas permeability for the five tested gases is increased by 26–45% at a 10 wt % zeolite loading and up to around 94–126% at a 20 wt % zeolite loading. Very interestingly, the CH_4 permeability can be enhanced by 3.5 times and the N_2 permeability can be enhanced by 2.8 times when the zeolite loading is increased to 30 wt %. These results suggest that the polymeric membrane structure changes after being embedded into β-zeolite particles, and this possibly leads to the formation of voids around zeolite particles at high zeolite loadings. Thus, the permeate molecules may readily and indiscriminately transport through the relatively loose membrane barrier in comparison with the pure polymer membrane. Therefore, SEM examinations of the morphologies of these β-zeolite-embedded PI membranes were made, and the SEM images are shown in Figure 5. As we can see, the β-zeolite particles are well distributed rather than conglomerated in the whole PI matrix, and this is indicative of the feasibility of the solution-casting technique employed. However, the SEM images also reflect that the interfacial region around some β-zeolite particles appears to form a loose structure or is even a void, plausibly resulting in a gaseous bypass between the glassy polymer chains and embedded β-zeolite particles. The loose structure throughout the whole membrane matrix is believably due to the partial incompatibility of the polymer chains and zeolite particles, indicating the weak interactions between the polymer and the zeolite framework. At high zeolite loadings, lots of voids might be created around zeolite particles, resulting in the porous structure and so increasing the permeating rate of all gases. Similarly, cavelike microporous structures, formed at high zeolite loadings (>30 wt %), have been reported for some zeolite-incorporated composite membranes.[22,23]

Table II presents the ideal permselectivities of the PI composite membranes for five gas pairs (He/N_2, O_2/N_2, CO_2/CH_4, He/O_2, and CO_2/N_2). Similar to PE (discussed previously), another term, selectivity enhancement (SE), is defined for facilitating the comparison study:

$$SE = \frac{S_{CM} - S_{polym}}{S_{polym}} \quad (4)$$

TABLE I
Permeability of the β-Zeolite–PI Composite Membranes at 35°C

Membrane	He	O_2	N_2	CH_4	CO_2
PI	22.2	1.68	0.254	0.194	6.5
PI-10	30.2 ± 0.3	2.25 ± 0.06	0.322 ± 0.021	0.278 ± 0.012	9.42 ± 0.14
PE (%)	36.0	33.9	26.8	43.3	44.9
PI-20	43.1 ± 0.2	3.65 ± 0.09	0.573 ± 0.024	0.422 ± 0.015	13.4 ± 0.3
PE (%)	94.1	117.3	125.6	117.5	106.2
PI-30	51.3 ± 0.5	4.16 ± 0.10	0.972 ± 0.032	0.882 ± 0.021	16.4 ± 0.2
PE (%)	131.1	147.6	282.7	354.6	152.3

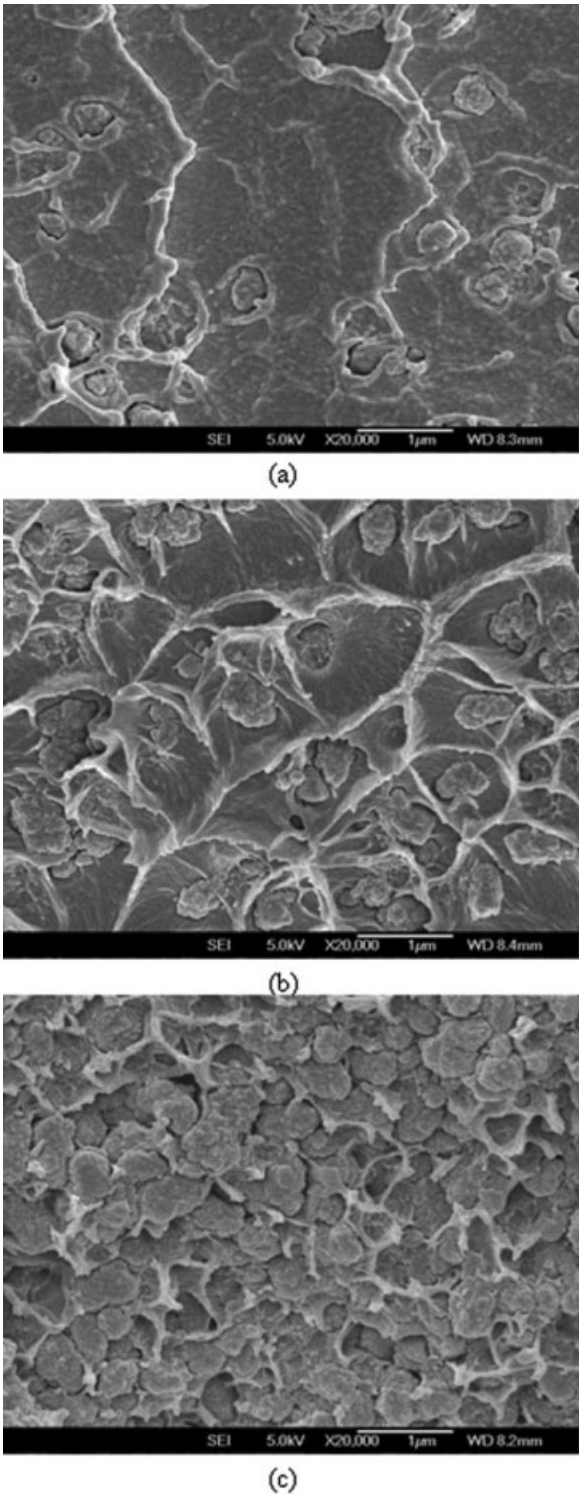

Figure 5 Cross-sectional SEM images of the β-zeolite–PI composite membranes at different zeolite loadings: (a) 10, (b) 20, and (c) 30 wt %.

where S_{polym} and S_{CM} are the ideal selectivities for the same gas pair in the neat polymer membrane and the zeolite-embedded composite membrane, respectively. A negative value of SE implies a decrease in the ideal selectivity of a gas pair in the zeolite–polymer composite membrane with respect to that of the neat polymer membrane (selectivity diminution). Contrary to the gas PE obtained previously, we have found that the ideal permselectivity values tend to drop after β-zeolite is embedded into the PI membrane. As shown in Table II, the composite membrane selectivities for four pairs are only around 55–66% of those of the neat PI counterparts at a zeolite loading of 30 wt %, and they slightly drop by about 5–14% at a zeolite loading of 20 wt %. These observations are mainly attributable to the presence of lots of voids around zeolite particles, arising from the unfavorable interaction between the polymer and zeolite phases. When the zeolite content in the matrix is 10 wt %, the values of α_{He/N_2}, $\alpha_{CO_2/N2}$, and $\alpha_{O_2/N2}$ are seen to improve by about 7, 14, and 6%, respectively. This slight increment in permselectivity may be related to the shape preference of β-zeolite, which possesses a sinusoidal channeling system.

Figure 6 shows Robeson plots for four gas pairs of industrial interest; they were obtained with the parameters proposed by Robeson[18] and Freeman.[24] As can be seen, the neat PI membrane is a promising candidate material for air separation as it provides an excellent compromise between O_2 permeability and O_2/N_2 selectivity. However, the polymer is somewhat far away from the upper-bound line for the other three gas pairs, as shown in Figure 6. Furthermore, the Robeson plots clearly show the effect of filled β-zeolite on the gas permeability and selectivity for the four gas pairs considered. The permeability versus selectivity point is closer to the upper-bound line as the zeolite loading increases, but it levels off or goes down with higher zeolite loadings (see Table II also). Overall, incorporating β-zeolite into the PI membrane subsequently results in highly increased gas permeability and relatively poor permselectivity. There are two possible reasons for these findings. One reason is the difference between the pore size of β-zeolite and the molecular size of these gases. β-Zeolite has a topographical uniform pore size of 7.1–7.3 Å,[1] and the gases in the experiments all have kinetic diameters much smaller than this pore size[20] and can diffuse through the pore

TABLE II
Ideal Permselectivity of the β-Zeolite–PI Composite Membranes at 35°C

Membrane	α_{He/N_2}	$\alpha_{O_2/N2}$	$\alpha_{CO_2/CH4}$	α_{He/O_2}	$\alpha_{CO_2/N2}$
Pure PI	87.4	6.61	33.5	13.2	25.6
PI-10	93.8	6.99	33.9	13.4	29.3
SE (%)	7.3	5.7	1.1	1.6	14.3
PI-20	75.2	6.37	31.8	11.8	23.4
SE (%)	−13.9	−3.6	−5.2	−10.6	−8.6
PI-30	52.8	4.28	18.6	12.3	16.9
SE (%)	−39.6	−35.3	−44.5	−6.7	−34.1

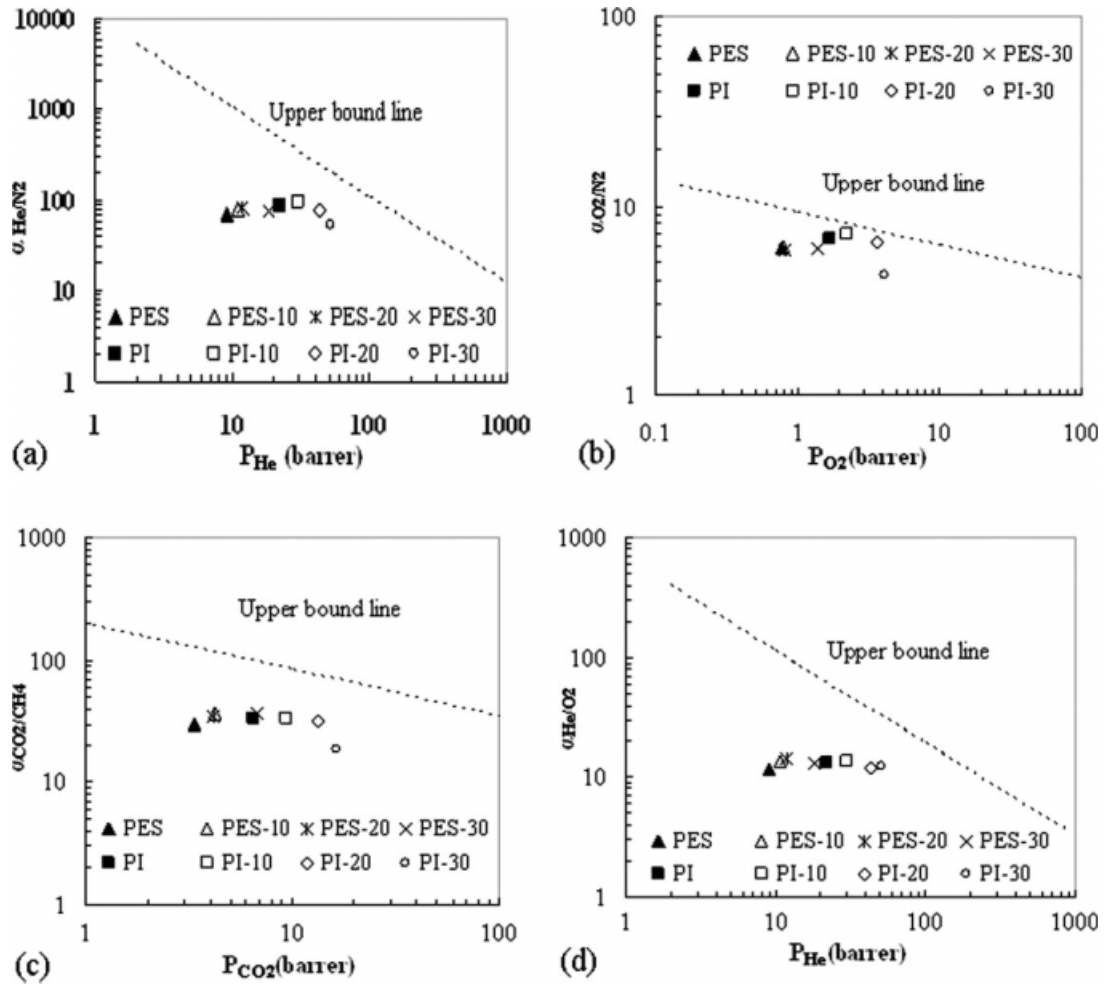

Figure 6 Robeson plots for several gas pairs of industrial interest: P_{He}, P_{O_2}, and P_{CO_2} are the permeability coefficient of a membrane to He, O_2, and CO_2, respectively.

structure easily; this subsequently leads to the increased permeability and decreased selectivity. The other reason is the possible presence of a no-selective region around zeolite particles as the organic PI matrix and inorganic fillers are different by nature; this may be the dominant reason at higher zeolite loadings for decreased gas separation performance. The organic–inorganic interfacial contact might be improved to some extent by heat treatment with the temperature over the polymer T_g or by a surface coating with silicone rubber.[12,13]

β-Zeolite–PES composite membranes

Table III lists the gas permeability values measured for a few PES composite membranes at different β-zeolite loadings. In comparison with the pristine PES dense membrane permeability, that of the PE membrane obtained with a 10 wt % zeolite loading is around 19 and 25% for He and CO_2, respectively. These values change slightly as the zeolite loading increases from 10 to 20 wt %. For the other three gases, the permeabilities remain almost the same as

TABLE III
Permeability of the β-Zeolite–PES Composite Membranes at 35°C

Membrane	He	O_2	N_2	CH_4	CO_2
Pure PES	9.10	0.773	0.129	0.112	3.38
PES-10	10.8 ± 0.1	0.806 ± 0.014	0.133 ± 0.006	0.114 ± 0.005	4.22 ± 0.10
PE (%)	18.7	4.3	3.1	1.8	24.9
PES-20	11.7 ± 0.2	0.825 ± 0.022	0.141 ± 0.008	0.121 ± 0.007	4.13 ± 0.09
PE (%)	28.6	6.7	9.3	8.0	22.2
PES-30	18.1 ± 0.3	1.39 ± 0.04	0.236 ± 0.014	0.186 ± 0.006	6.82 ± 0.12
PE (%)	98.9	79.8	82.9	66.1	101.8

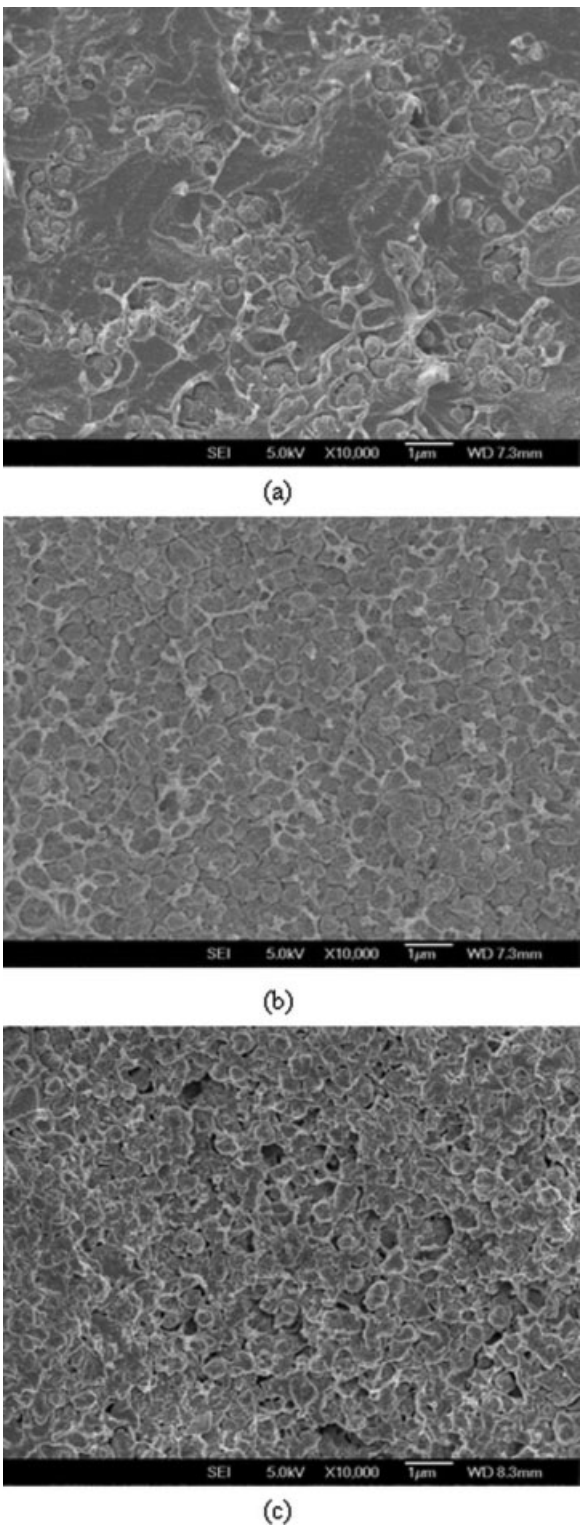

Figure 7 Cross-sectional SEM images of the β-zeolite–PES composite membranes at different zeolite loadings: (a) 10, (b) 20, and (c) 30 wt %.

those of the pure PES dense film with a 10 wt % zeolite loading, but they are slightly enhanced by about 6% at a 20 wt % zeolite loading. Considerably high gas permeabilities have been observed for all these gases at a 30 wt % zeolite loading. As shown in Table III, a 30 wt % zeolite loading results in the permeability being enhanced by 99, 80, 83, 66, and 102% for He, N_2, O_2, CO_2, and CH_4, respectively. These permeability increments may be related to the large pore size of β-zeolite and the packing looseness/compactness of the polymer chains and zeolite entities across the membrane. Figure 7 shows a cross-sectional view of the β-zeolite-embedded PES composite membrane. Zeolite particles can be observed to be uniformly dispersed in the PES substrate matrix. At different zeolite loadings, the β-zeolite particles and polymer matrix are closely packed with each other, and no obvious voids between the β-zeolite particles and PES can be found; this indicates rather good compatibility between the zeolite and polymer. These SEM observations are in good agreement with the heat treatment used. As described earlier, the heat treatment was carried out at 250°C, which is higher than the T_g of PES (ca. 220°C); this annealing may make the polymer molecules more flexible, and the chains readily rearrange around the zeolite particles and exclude the free volume retained. This subsequently results in the compact membrane structure, possibly leading to effective reduction of the voids induced by the zeolite phases. Therefore, the gas permeability improvement may primarily arise from the molecular sieving and preferential adsorption of zeolite entities. Table III also shows that the gas permeability increases in the sequence of $CH_4 < O_2 \approx N_2 < He \approx CO_2$; this agrees very well with the decreasing order of the gas kinetic dimensions:[20] He (2.60 Å) < CO_2 (3.30 Å) <O_2 (3.46 Å) < N_2 (3.64 Å) < CH_4 (3.80 Å). In addition to the diffusion aspects, which imply a faster permeation rate for smaller molecules such as He, the marked permeability increase of CO_2 may also be due to its pronounced adsorption on β-zeolite.[11]

Table IV presents the ideal selectivity of five pairs (He/N_2, CO_2/N_2, CO_2/CH_4, He/O_2, and O_2/N_2) for β-zeolite-incorporated PES composite membranes. For the O_2/N_2 gas pair, there is no permselectivity improvement achieved by zeolite filling, perhaps because the adsorption and diffusion parameters of

TABLE IV
Ideal Permselectivity of the β-Zeolite–PES Composite Membranes at 35°C

Membrane	α_{He/N_2}	$\alpha_{O_2/N2}$	$\alpha_{CO_2/CH4}$	α_{He/O_2}	$\alpha_{CO_2/N2}$
PES	70.5	5.99	30.2	11.8	26.2
PES-10	81.2	6.06	37.0	13.4	31.7
SE (%)	15.1	1.1	22.7	13.8	21.1
PES-20	83.0	5.85	34.1	14.2	29.3
SE (%)	17.6	−2.4	13.1	20.5	11.8
PES-30	76.7	5.89	36.7	13.0	28.9
SE (%)	8.7	−1.7	21.5	10.6	10.3

O_2 and N_2 for β-zeolite are close to each other.[11] As shown in Table IV, the permselectivity enhancement varies in the range of 8.7–22.7% for the other three pairs. These resultant selectivity data further confirm that at least some penetrant molecules have permeated through the zeolite pores and channels to transport across the composite membrane. Thus, the interaction between the penetrant and the zeolite framework may have affected the membrane separation performance. Because of the high quadrupole moment of CO_2 and high polarizability of methane, these two gases show certain interactions with the heterogeneous surface of β-zeolite. Thus, the adsorption affinity of gases to β-zeolite is $O_2 \approx N_2 < CH_4 < CO_2$.[11] As a result of combined adsorption and diffusion aspects of embedded zeolites, a permselectivity increase can be achieved for these gas pairs.

Robeson plots, shown in Figure 5, were also made for β-zeolite–PES composite membranes. As we can see, the neat polymer is quite far away from the upper-bound line for the four gas pairs. After the zeolite is introduced into the polymer, the permeability–selectivity plot for all gas pairs appears to be closer to the upper-bound line, but to a very limited degree. In particular, the selectivity for the CO_2/CH_4 pair is not good as expected and much poorer than that previously reported.[15] Thus, it may not be easy to break through the upper-bound line by the simple incorporation of zeolite into a promising polymer, and more effort should be made in future research.

Comparison of different composite membranes

An examination of Tables II and III reveals that after the incorporation of the same β-zeolite, PI exhibits a pronounced gas permeability increase but slightly lower permselectivities at a low zeolite loading and greatly decreased ones at higher zeolite loadings, and PES shows an obvious increase in both the permeability and selectivities but considerably increased permeability at high zeolite loadings. A possible explanation is that the annealing temperature used is much lower than the T_g of PI and subsequently results in rather loose membranes.[12,13] Interestingly, it may be economically meaningful, through the use of β-zeolite to modify the PI properties at an appropriate loading, to significantly improve the productivity (i.e., the permeability) by twofold but at a very small cost to gas permselectivity.

A comparison made with the literature[12,13] shows that the separation performances achieved for these PES composite membranes are very consistent with those of dual-layer hollow-fiber membranes through the embedding of β-zeolite into the PES matrix,[12] being similar to those obtained by the incorporation of β-zeolite into polysulfone.[13] However, the selectivity improvement of less than 30% obtained in these studies is much lower in comparison with that reported by Falabella and Bac,[15] who wrote that a PES membrane containing 17 wt % β-zeolite exhibited an ideal selectivity in favor of CO_2 over CH_4 6 times greater than that of pure PES. This selectivity value for CO_2/CH_4 is surprisingly close to the adsorption equilibrium separation selectivity of 8–26 reported for β-zeolite particles at 40–100°C.[11] In our earlier work, a zeolite A-incorporated PES membrane showed pronounced permeability decompression but considerably increased gas permselectivities.[20] The differences in the permeation property may be not only due to the nature of zeolites added but also due to the fact that the polymer chain molecules experience a different packing revolution after the incorporation of zeolite particles, as reflected by the morphology and internal structure of these composite membranes achieved through SEM observations. In light of these observations, the zeolite characteristics, such as the selective diffusion and preferential adsorption, the composite membrane casting method, and the zeolite–polymer interfacial properties must be considered to better understand the gas permeation mechanism and favorably improve the separation performance of these zeolite-incorporated composite membranes.

CONCLUSIONS

In this study, we fabricated several β-zeolite-embedded polymer composite membranes by means of the solution-casting method. The membrane performance was evaluated with respect to the gas permeability and permselectivity. The following conclusions can be drawn from this study:

1. After the incorporation of β-zeolite particles, the PI membrane exhibited a striking increase in the gas permeability but a considerable decrease in the permselectivity, and this was attributed to the presence of the loose structure and gaseous bypass created around β-zeolite particles, as shown by SEM observations.
2. The addition of β-zeolite to the PES membrane resulted in obvious increases in both the gas permeability and selectivities, mainly because of the pore size sieving and preferential adsorption of β-zeolite entities. The annealing heat treatment at a temperature over T_g may have resulted in the formation of the closely packed composite membrane structure, as examined by SEM analysis.
3. The zeolite loadings induced significant changes in both the permeability and selectivity. The PI composite membrane exhibited a pronounced gas permeability increase but decreased selectivities as the zeolite loading increased. In the case

of the PES membranes, the permeability increase was considerable at high zeolite loadings, but the increase in the selectivity was not strongly relevant to the zeolite content. The Robeson plots showed that the performances of these composites membranes promisingly approached the upper-bound line. However, the permeability/selectivity data obtained still could not break through the Robeson upper bound.

4. A comparison of different composite membranes involved in the incorporation of β-zeolite particles implies that the changes in the membrane gas separation performance not only are attributable to the properties and content of β-zeolite particles but also depend on the heterogeneous microstructure created around the zeolite entities. Thus, more investigations are necessary to further improve the interfacial properties between the polymer and the zeolite sieves to achieve the integral properties of polymer–zeolite composite materials.

The authors thank T. S. Chung, Y. Li, and L. Y. Jiang at the National University of Singapore for their comments and assistance with the experimental gas permeation setup and data analysis.

References

1. Breck, D. W. Zeolite Molecular Sieves; Wiley: New York, 1964.
2. Cervený, L.; Mikulcová, K.; Cejka, J. Appl Catal A 2002, 223, 65.
3. Halgeri, A. B.; Das, J. Appl Catal A 1999, 181, 347.
4. De Angelis, P. I.; Perego, C. Ind Chem Eng Res 2004, 43, 1169.
5. Corma, A.; Nemeth, L. T.; Renz, M.; Valencia, S. Nature 2001, 412, 423.
6. Tuan, V. A.; Li, S. G.; Falconer, J. L.; Noble, R. D. Chem Mater 2002, 14, 489.
7. Maloncy, M. L.; van den Berg, A. W. C.; Gora, L.; Jansen, J. C. Microporous Mesoporous Mater 2005, 85, 96.
8. Shao, G. L.; Yang, J. H.; Zhang, X. F.; Zhu, G.; Wang, J. Q.; Liu, C. Mater Lett 2007, 61, 1443.
9. Denayer, J. F.; Souverijns, W.; Jacobs, P. A.; Martens, J. A.; Baron, G. V. J Phys Chem B 1998, 102, 4588.
10. Huddersman, K.; Klimczyk, M. AIChE J 1996, 42, 405.
11. Li, P. Y.; Tezel, F. H. Microporous Mesoporous Mater 2007, 98, 94.
12. Li, Y.; Chung, T. S.; Huang, Z.; Kulprathipanja, S. J Membr Sci 2006, 277, 28.
13. Jiang, L. Y.; Chung, T. S.; Kulprathipanja, S. J Membr Sci 2006, 276, 113.
14. Jiang, L. Y.; Chung, T. S.; Rajagopalan, R. Carbon 2007, 45, 166.
15. Falabella, J. B.; Bac, N. In Proceedings of the North American Membrane Society 13th Annual Meeting, Long Beach, CA; The North American Society: Toledo, Ohio, May 2002; p 94.
16. Chung, T. S.; Jiang, L. Y.; Li, Y.; Kulprathipanja, S. Prog Polym Sci 2007, 32, 483.
17. Huang, Z.; Guan, H. M.; Tan, W. L.; Qiao, X. Y.; Kulprathipanja, S. J Membr Sci 2006, 276, 260.
18. Robeson, L. M. J Membr Sci 1991, 62, 165.
19. Huang, Z.; Luan, D. Y.; Shen, S. C.; Hidajat, K.; Kawi, S. J Supercrit Fluids 2005, 35, 40.
20. Huang, Z.; Li, Y.; Wen, R.; Teoh, M. M.; Kulprathipanja, S. J Appl Polym Sci 2006, 101, 3800.
21. Ding, L. H.; Zheng, Y. Microporous Mesoporous Mater 2007, 103, 94.
22. Süer, M. G.; Baç, N.; Yilmaz, L. J Membr Sci 1994, 91, 77.
23. Gür, T. M. J Membr Sci 1994, 93, 283.
24. Freeman, B. Macromolecules 1999, 33, 375.